Eumelanin-Coated Aligned PLA Electrospun Microfibers to Guide SH-SY5YCells Spreading, Alignment, And Maturation

Anna Mariano, Ines Fasolino, Nikita Bhupesh Dinger, Claudia Latte Bovio, Irene Bonadies, Alessandro Pezzella, Luigi Ambrosio, Maria Grazia Raucci,* and Francesca Santoro*

During the development of the nervous system, neurons sense and respond to topographical and biochemical cues found in the brain's native environment. Such niche-specific cues are pivotal for neural tissue formation and development and have been now widely exploited in neural tissue engineering to develop biologically-inspired scaffolds able to trigger a desired neuronal behavior. In particular, anisotropic aligned fibers, recapitulating the design of extending axonal tracts or aligned fibers found in the extracellular environment, have emerged as ideal candidates to guide cell alignment and elongation along the substrate main axis as well as promote neuronal differentiation. Among natural polymers used for coatings, melanins, including eumelanin, have been shown to possess antioxidant, anti-inflammatory, immunomodulatory, and photo-protective properties. Here, aligned poly(lactic acid) (PLA) fibers are fabricated via electrospinning and then coated with eumelanin via spin coating. Eumelanin-coated aligned PLA fibers are highly biocompatible and greatly influenced the adhesion, morphology, and spreading of SH-SY5Y neuroblastoma cells. Furthermore, the eumelanin coating is crucial in promoting cell alignment at the cell-material interface and SH-SY5Y cell maturation towards a more mature neuronal phenotype.

1. Introduction

Neural tissue engineering requires the fabrication of biocompatible scaffolds whose chemical and topographical properties can be tailored to dictate cell function and fate.[1–3] In particular, biologically-inspired topographical cues have been now widely employed as cell-instructive materials to tune a desired cell behavior at the cell-material interface.[4–8] Among these, anisotropic substrates represent a promising tool to develop scaffolds suitable for neural repair strategies.[9–14] In particular, inspired by the shape and geometries of fibers and fibrils found in the extracellular environment (e.g., axonal tracts and bundles of extending neurites), anisotropic aligned fibers become the ideal candidate to dictate neurite alignment and elongation along the substrate main axis as well as promoting neuronal differentiation.[15–20]

A. Mariano, N. B. Dinger, C. Latte Bovio, F. Santoro
Tissue Electronics
Istituto Italiano di Tecnologia
80125 Naples, Italy
E-mail: f.santoro@fz-juelich.de

I. Fasolino, L. Ambrosio, M. G. Raucci
Institute of Polymers
Composites and Biomaterials (IPCB) – CNR
Viale J. F. Kennedy 54, Mostra D'Oltremare Pad 20, Naples 80125, Italy
E-mail: mariagrazia.raucci@cnr.it

N. B. Dinger, C. Latte Bovio
Dipartimento di Ingegneria Chimica
dei Materiali e delle Produzioni Industriali
DICMAPI
Università 'Federico II'
80125 Naples, Italy

I. Bonadies, A. Pezzella
Institute of Polymers
Composites and Biomaterials (IPCB) – CNR
Via Campi Flegrei 34, 80078 Pozzuoli, Italy

A. Pezzella
Department of Physics "Ettore Pancini"
University of Naples "Federico II"
Via Cintia 4, IT-80126 Naples, Italy

A. Pezzella
Bioelectronics Task Force
University of Naples Federico II
80126 Naples, Italy

F. Santoro
Faculty of Electrical Engineering and Information Technology
RWTH Aachen
52074 North Rhine-Westphalia, Germany

F. Santoro
Institute for Biological Information Processing- Bioelectronics
IBI-3
Forschungszentrum Juelich
52428 Jülich, Germany

Among biocompatible materials for fibers fabrication, polylactide (PLA) electrospun fibers are often used in tissue engineering,[20,21] neural repairs strategies[22–24] and neural stem cell differentiation.[20,25] Importantly, PLA fibers might be coated with natural bioactive molecules in order to modulate their surface properties (e.g., hydrophobicity, adhesivity), and ultimately their influence on cells interfacing.[26] Among natural polymers, eumelanin-based blends and coatings have now been widely used for the fabrication of innovative multifunctional biointerfaces,[27–29] ensuring cells adhesion[30,31] and good biocompatibility.[32] Specifically, eumelanins – the major class of natural organic semiconductors – derived biogenetically from the oxidative polymerization of 5,6-dihydroxyindole (DHI) and 5,6-dihydroxyindole-2-carboxylic acid (DHICA) have been the focus of continuing interest due to their key properties: a broadband featureless optical absorption throughout the entire UV–vis range accounting for their black color, nearly quantitative non-radioactive conversion of absorbed photon energy, photoconductivity in the solid state, electronic-ionic hybrid conductor properties, hydration-dependent free radical properties, metal ion-binding properties and redox behavior.[27,28] In addition, eumelanin ensures other characteristics useful for the realization of bioelectronics devices: chemical stability and unwanted side reactions in biological environment are particularly important for chronic implantable devices; as well as, the ability to engineer their chemical structure to tune such solid-state properties alongside the possibility to integrate them with other functional materials- proteins or carbon nanostructures – to realize blends or hybrids, make the fabrication of multifunctional bioelectronic devices with different geometries less technically challenging.

Eumelanin blends and hybrids have been recently developed paring the pigment with classical conductive polymers such as PEDO:PSS[33] to gain adhesion and water stability as well as carbon nanostructure (CNS) to improve electronic conductivity.[34] Such scaffolds were able to commit multipotent stem cells toward a neuronal lineage even in the absence of exogenous neurotrophins, highlighting their biomimetic potential.[35] Beyond this, bio-glasses[36] have been developed to address biocompatibility and/or bioresorbability and replace silicon dioxide glass which has the drawback of being hazardous for in vivo applications. Bio-glass-based optical fibers can be used to integrate multiple functionalities to substrates:[37] by using different configurations, light can be both focused on precise spots and distributed along the length of the fiber itself. The combination of these features with an organic biocompatible electric conductor element such as eumelanin could represent a breakthrough to deliver/read light and electric signals at the same time from cells or even, in perspective, organoids. In the context of cell-replacement therapies, a promising source of cells is the direct cell-reprogramming technology (or trans-differentiation) that allows to convert adult somatic cells into different cell types.[38] In addition, during tissue regeneration phases, organoid formation shows limitations such as organoid size as well as proper compartmentalization and tissue organization. All these limitations can be overcome by using smart eumelanin-based biointerfaces that can induce differentiation through inducing or reprogramming factors, support organoid formation, and facilitate the reprogramming of somatic cells. Ideally, these interfaces, under the effects of external stimuli (i.e., electrical, optical), should be able to permit crosstalk with cells establishing a series of feedback loops aimed at directing cell behavior.

Furthermore, among pharmacological activities, eumelanin also possesses antioxidant, anti-inflammatory, immunomodulatory, and photo-protective properties.[39–41] In addition, eumelanin has drawn a lot of attention as a functional material for bioelectronics and optoelectronic applications owing to its ionic-to-electronic mixed conductivity.[42] Notably, random and low-density aligned eumelanin-coated PLA fibers were recently fabricated combining the electrospinning technology and 5,6-dihydroxyindole (DHI) solid-state polymerization[43] and used for embryonic stem cell differentiation.[32] These microfibers have been shown to support SH-SY5Y cell growth and adhesion as well as promote their differentiation toward a more mature neuronal phenotype.[35]

Here, in order to further investigate the potential of eumelanin-coated PLA fibers as a cell culture platform able to guide cell directionality in a newly formed neuronal tissue, the microfibers' effects on cell adhesion, spreading, and maturation were evaluated. For that reason, the fibers were synthesized as previously reported in Fasolino et al.,[35] but with increased density (#/μm = 0.9). The biocompatibility of such substrates and their effect on proliferation was evaluated using human-derived SH-SY5Y neuroblastoma cells. In this work, a more detailed characterization of cell-fiber interactions at the interface was carried out by investigating SH-SY5Y cell adhesion, morphology, and spreading on both coated and uncoated aligned PLA fibers by means of focused ion beam/scanning electron microscopy methodology (FIB/SEM). The ability of eumelanin-coated and uncoated aligned PLA fibers to guide cell alignment at the cell-material interface was then further investigated by means of fluorescence microscopy. Finally, the influence of the high-density microfibers used on SH-SY5Y differentiation into a more mature neuronal phenotype was assessed. Our results, shedding light on the combinatorial effects of eumelanin-based coatings and aligned PLA fibers on neuronal cell adhesion, spreading, and maturation, may contribute to deepening our knowledge of how substrates properties can be specifically tailored to dictate a desired cellular behavior at the interface in order to develop scaffolds suitable for neural tissue engineering and bioelectronics applications.

2. Results and Discussion

2.1. PLA and EU@PLA Fibers are Biocompatible and Support SH-SY5Y Cell Proliferation

PLA microfibers were synthesized via gap electrospinning as previously reported in Fasolino et al., but with increased fiber density, and then coated via spin coating starting from a DHI solution under a nitrogen atmosphere.[35] In particular, the number of fibers within a fixed distance orthogonal to the fiber alignment direction (#/μm) was increased from 0.7 to 0.9.[35]

ADVANCED
Science News
www.advancedsciencenews.com

ADVANCED
MATERIALS
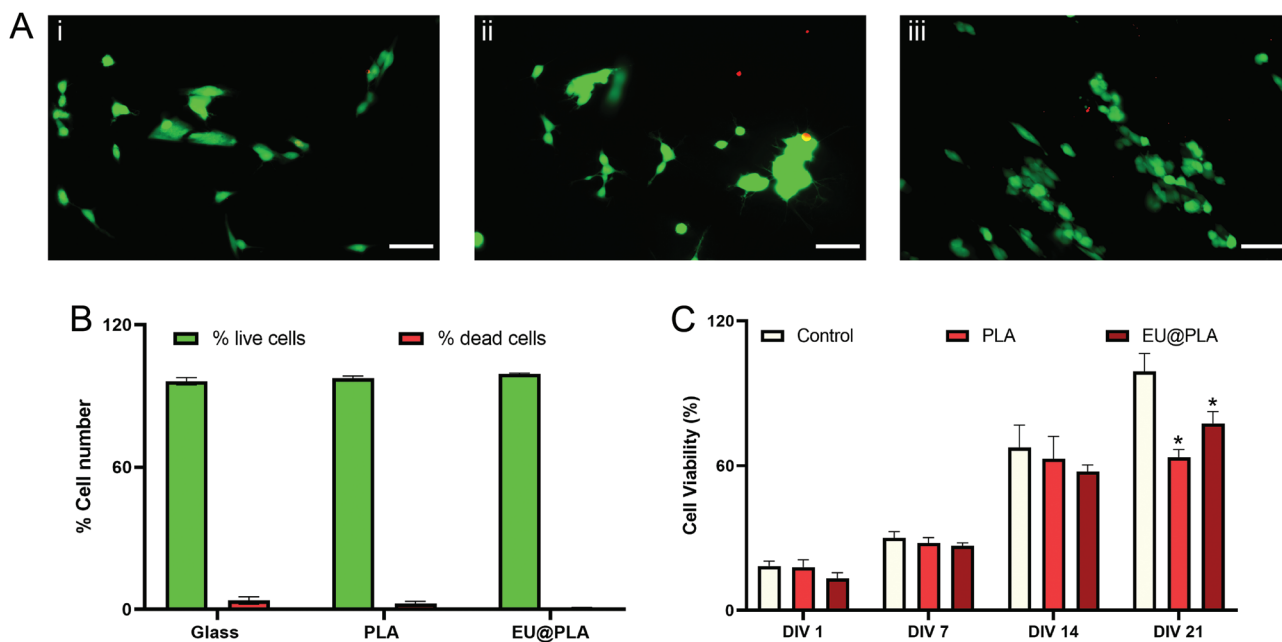**INTERFACES**
Open Access
www.advmatinterfaces.de

Figure 1. SH-SY5Y cells viability and proliferation on PLA and EU@PLA fibers. A) Cell viability assay showing fluorescently labeled live (green) and dead (red) cells on i) control, ii) PLA fibers, and iii) EU@PLA fibers. Scale bar 50 µm. B) Percentage of live and dead cells reported as mean ± SEM ($n = 3$). One-way ANOVA test with post hoc Dunnett's test. C) Cell proliferation at DIV 1, DIV 7, DIV 14, and DIV reported as mean ± SEM ($n = 3$). One-way ANOVA test with post hoc Dunnett's test. *$p < 0.05$; **$p < 0.01$.

In order to assess the biocompatibility of the newly synthesized aligned PLA fibers with and without the eumelanin coating with SH-SY5Y cells, a live/dead fluorescence assay was performed after 1 day in vitro (DIV). The green fluorescent signal of live cells labeled with Calcein-AM and the red fluorescent signal of dead cells labeled with ethidium homodimer (**Figure 1**A) were used to quantify cell viability (Figure 1B). SH-SY5Y cells displayed excellent viability on both PLA and EU@PLA fibers, with a high percentage of live cells (above 97%) comparable to the percentage measured for glass control samples. In addition, no significant difference in the percentage of live cells was found between coated or uncoated PLA fibers, indicating that they all display negligible cytotoxic effects irrespective of the presence of the eumelanin coating. These results agree with previous works on PLA[44] and eumelanin[31] biocompatibility.

To further investigate the ability of PLA and EU@PLA fibers to support cells' growth and their proliferation over culture time, an Alamar blue assay was performed on SH-SY5Y cells seeded on PLA and EU@PLA at DIV 1, 7, 14, and 21.

No significant differences in cell proliferation were observed between glass control, PLA, and EU@PLA at DIV 1, DIV 7, and DIV 14 (Figure 1C). Conversely, a significant reduction in cell proliferation was observed at DIV 21 on PLA and EU@PLA fibers compared to glass (Figure 1C). This is in agreement with previous works showing that both random and aligned EU@PLA fibers promote cell differentiation and consequently a reduction of the cells' proliferation rate.[35]

The proliferation rate did not differ between coated and uncoated aligned PLA fibers over culture time (Figure 1C). This suggests that the reduction in cell proliferation observed at DIV

21 on both materials is mediated by the topographical cues provided by the fibers.

2.2. EU@PLA Fibers Dictate Cell Alignment at the Cell-Material Interface

Aligned fibers have been widely used in neural tissue engineering applications owing to their ability to guide cell alignment and neurite extension through contact-guidance processes at the cell-material interface.[45,46] To better understand the role of the eumelanin coating in guiding cell alignment, SH-SY5Y cells seeded on PLA and EU@PLA fibers and their cytoskeleton and nuclei were fluorescently labeled against FITC-conjugated phalloidin (in green) and 4′,6-diamidino-2-phenylindole (DAPI, in blue), respectively, at DIV 7 (**Figure 2**A). Interestingly, SH-SY5Y cells more closely follow and spread on PLA fibers when these are coated with eumelanin, showing unidirectional growth. By contrast, cells on uncoated PLA fibers displayed an anisotropic growth (Figure 2A). These results were further confirmed by the directionality analysis performed on SH-SY5Y cells seeded on both PLA and EU@PLA fibers (Figure 2B). Here, the histogram of fast Fourier transform (FFT) analysis of cell directionality was used to infer the preferred orientation of cells on both substrates. The histogram indicates a clear peak (around 90°) for cells cultured on EU@PLA fibers (Figure 2B). Conversely, SH-SY5Y cells cultured on uncoated PLA fibers do not show a preferred orientation. This results in a flat histogram with multiple peaks at random angles of the histogram (Figure 2B). Taken together these results suggest that eumelanin may indeed be pivotal in establishing oriented cell growth at the cell material interface.
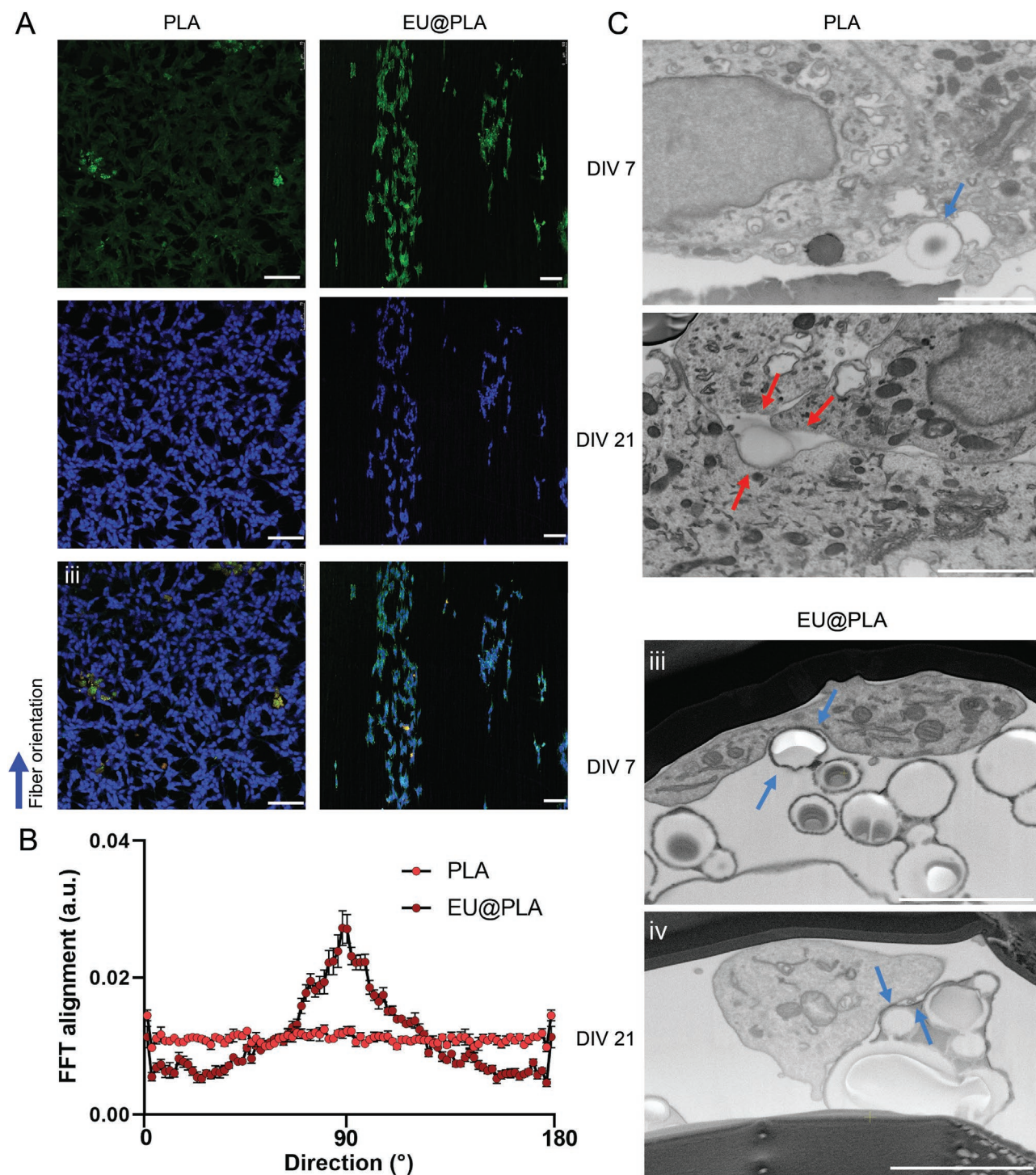
**ADVANCED
SCIENCE NEWS**

www.advancedsciencenews.com

**ADVANCED
MATERIALS
INTERFACES**

www.advmatinterfaces.de

Figure 2. SH-SY5Y cells alignment on PLA and EU@PLA fibers. A) Fluorescence images of SH-SY5Y cells on PLA and EU@PLA fibers. Cells were fluorescently labeled for the nuclei (blue) and FITC-phalloidin (green). Scale bar 100 μm. B) Histogram of directionality, based on the Fast Fourier transform analysis, of cells cultured on both substrates reported as mean ± SEM. C) FIB/SEM showing cell-fiber interaction of SH-SY5Y cells cultured on PLA at i) DIV 7 and ii) DIV 21 and on EU@PLA substrates at iii) DIV 7 and iv) DIV 21. Scale bar 2 μm.

2.3. EU@PLA Fibers Influence Cell Morphology and Spreading

The contact area between SH-SY5Y cells and the imposed topography was then visualized by means of SEM and in situ cross-sectioning by focused ion beam milling (Figure 2C). On both coated and uncoated PLA fibers, the plasma membrane tightly follows the fibers profile, suggesting that cells are actively interacting with the imposed topography at both
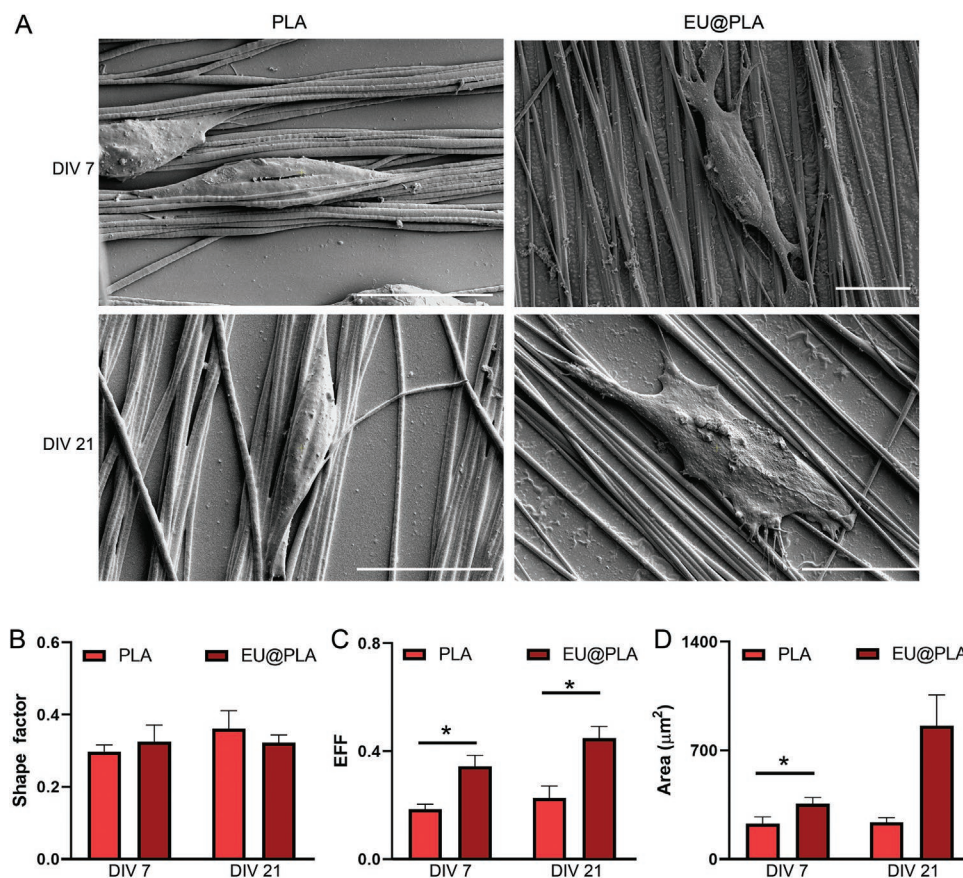
2202022 (4 of 10)

ADVANCED
SCIENCE NEWS
www.advancedsciencenews.com

ADVANCED
MATERIALS
INTERFACES
Open Access
www.advmatinterfaces.de

Figure 3. SH-SY5Y cells spreading, elongation, and adhesion on PLA and EU@PLA fibers. A) Top-view scanning electron micrographs showing top-view SH-SY5Y cells on PLA and EU@PLA fibers at DIV 7 and DIV 21. Scale bar 20 μm. B) Shape factor reported as mean ± SEM. C) EFF reported as mean ± SEM. D) Area reported as mean ± SEM. Unpaired Student's t-test, $*p < 0.05$.

DIV 7 and DIV 21 (red and blue arrows, Figure 2C). FIB-SEM micrographs also show that as cells spread and elongate to explore the substrate underneath, their membrane can either wrap around (blue arrows) or envelop (red arrows) fibers (Figure 2C). The increased surface available for cell-material interactions may be pivotal in regulating the topography-driven changes in cell morphology and spreading observed on the microfibers.[4,47]

The topographical features of electrospun fibers play a key role in regulating cell behavior at the interface, including adhesion, morphology, spreading, and elongation.[48–50] To further investigate the combinatorial effect of the topographical arrangement of the substrate and the eumelanin coating in mediating cell-substrate interaction, the morphology of SH-SY5Y cells on both PLA and EU@PLA aligned fibers was analyzed by means of scanning electron microscopy (SEM) at DIV 7 and DIV 21 (**Figure 3**A).

Morphological characteristics of cells plated on both PLA and EU@PLA fibers were evaluated through the assessment of different parameters: the shape factor, defined as $4\pi A/P^2$ (where A and P are the cellular area and perimeter, respectively), the elliptical form factor (EFF), defined as the major axis divided by the minor axis, and the cell area (Experimental Section).[51] The

shape factor quantifies how rounded a cell is and its value may range from 0 to 1. A shape factor equal to 1 means that a cell is perfectly circular, whereas a shape factor closer to zero indicates that such symmetry is lost. The shape factor was close to 0 for cells on both PLA and EU@PLA fibers (Figure 3B). Such a low value is in agreement with the spindle-shaped morphology of SH-SY5Y cells observed on both PLA and EU@PLA fibers (Figure 3A). Furthermore, the shape factor did not statistically vary across substrates at DIV 7 or DIV 21 days, indicating that both coated and uncoated fibers are able to influence SH-SY5Y cell morphology (Figure 3B). Relevantly, SH-SY5Y cells cultured on EU@PLA displayed a significant increase in EFF and area at DIV 7 and a significant increase in EFF at DIV 21 (Figure 3C,D). If both coated and uncoated fibers encouraged cells to assume a spindle-shaped morphology, the presence of the eumelanin coating appears to further incentivize cell elongation and spreading on coated fibers. In addition, top-view micrographs of SH-SY5Y cells cultured on EU@PLA fibers show the formation of membrane protrusions involved in substrate tethering at the cell-material interface.[52–54] These findings suggest that the presence of the eumelanin coating may encourage SH-SY5Y cells to actively explore their surroundings, resulting in an increased area and a more spread morphology (Figure 3A).
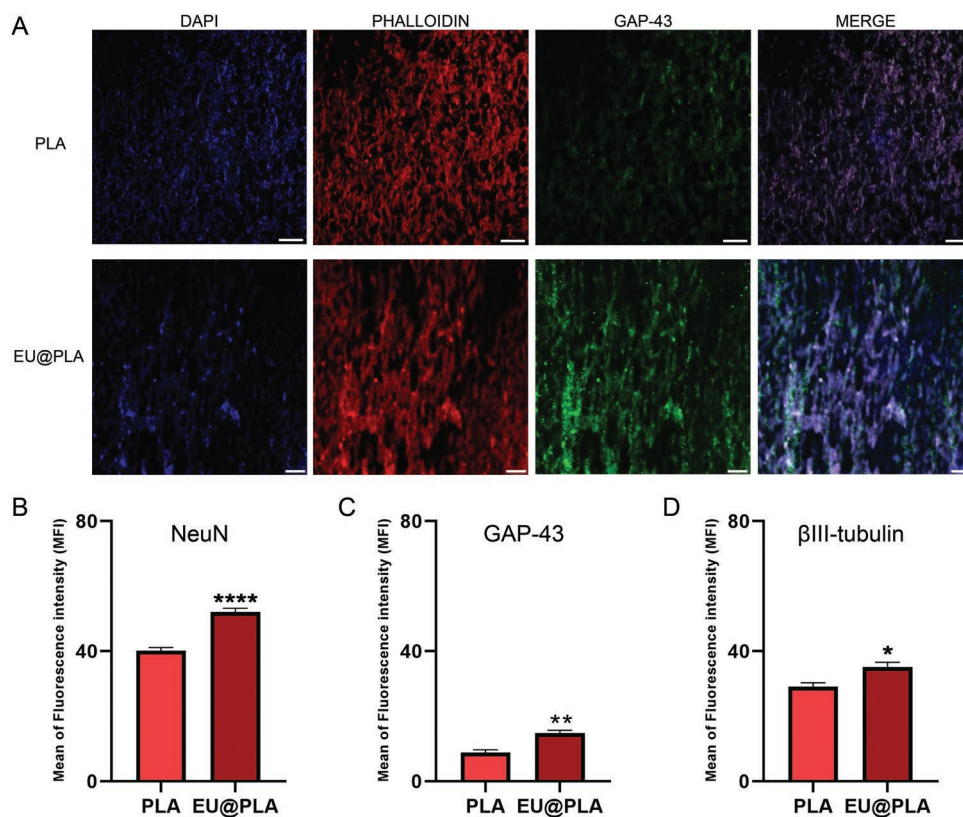
Figure 4. SH-SY5Y cells maturation on PLA and EU@PLA fibers. A) Fluorescence images of SH-SY5Y cells on PLA and EU@PLA fibers at DIV 21. Cells were fluorescently labeled for the nuclei (blue), rhodamine-phalloidin (red), and GAP-43 (green). Scale bar 50 μm. Mean fluorescence intensity of B) NeuN, C) GAP-43, and D) βIII-tubulin reported as mean ± SEM (n = 3). Unpaired Student's t-test, * $p < 0.05$; ** $p < 0.01$; **** $p < 0.0001$.

2.4. PLA and EU@PLA Fibers Promote SH-SY5Y Cells Differentiation

Previous works have shown that only eumelanin-coated random and aligned PLA fibers promote SH-SY5Y cells differentiation towards a more mature neuronal phenotype. However, aligned EU@PLA with a lower fiber density (#/μm = 0.7) did not exert the same effect on cell maturation.[35] Here, the ability of high-density aligned PLA fibers (#/μm = 0.9) with and without the eumelanin coating to promote SH-SY5Y cell differentiation and the cytoskeletal organization supporting neuronal maturation were evaluated (**Figure 4**A–D). First, the expression levels of two markers nestin and NeuN were evaluated. Nestin, an intermediate filament protein, is mainly expressed in undifferentiated cells and is replaced by neuron-specific proteins as cells differentiate into neurons.[55,56] NeuN is a protein localized in the nuclei and perinuclear cytoplasm of differentiated neurons and, is most frequently used as a neuronal differentiation marker.[57] SH-SY5Y cells cultured on PLA and EU@PLA fibers were fluorescently labeled against nestin (in red) and NeuN (in green) at DIV 21 (Figure S1A, Supporting Information). Relevantly, on eumelanin-coated PLA fibers, the expression levels of both nestin and NeuN are significantly increased compared to uncoated fibers (Figure S1B, Supporting Information and Figure 4B), indicating that the presence of the eumelanin coating does encourage cells differentiation towards a more mature neuronal phenotype as previously observed on random

PLA fibers.[35] However, SH-SY5Y cells are not completely differentiated. This was further confirmed by the decreased proliferation rate of SH-SY5Y cells on eumelanin-coated fibers at DIV 21, suggesting that despite cells differentiating towards a more mature neuronal phenotype and withdrawing from the cell cycle, they still maintain the ability to proliferate (Figure 1C).[58–60]

In previous work, SH-SY5Y cell maturation on eumelanin-coated random PLA fibers was accompanied by increased expression levels of growth-associated protein 43 (GAP43).[35] GAP-43 is a protein found in developing neuronal growth cones and regenerating axons[61] and whose expression coincides with the beginning of neurite outgrowth.[62] For this reason, SH-SY5Y cells cultured on aligned PLA and EU@PLA fibers were fluorescently labeled against nuclei (in blue), phalloidin (in red), and GAP-43 (in green) at DIV 21 (Figure 4A). Relevantly, GAP-43 expression levels were significantly increased on eumelanin-coated fibers (Figure 4C), indicating that the presence of the eumelanin coating is essential in promoting SH-SY5Y cell maturation.

Differentiating neurons are characterized by a more complex cytoskeletal organization which has to provide adequate support.[63] In order to investigate the cytoskeletal architecture supporting SH-SY5Y cell neuronal maturation, cells cultured on PLA and EU@PLA fibers were fluorescently labeled against microtubule-associated protein 2 (MAP-2) (in green) and βIII-tubulin (in red) at DIV 21. Both MAP-2 and βIII-tubulin are

**ADVANCED
SCIENCE NEWS**

www.advancedsciencenews.com

**ADVANCED
MATERIALS
INTERFACES**

www.advmatinterfaces.de

two well-known cytoskeletal markers with neuron specificity (Figure S2A, Supporting Information).[64] The expression levels of both MAP-2 and βIII-tubulin were significantly increased on eumelanin-coated fibers (Figure S2B, Supporting Information and Figure 4D). This is in agreement with previous observations in which SH-SY5Y cell neuronal differentiation on random fibers was accompanied by an increased expression of these two markers.[56]

3. Conclusion

In this work, the potential of biologically-inspired aligned PLA fibers coated with eumelanin to influence SH-SY5Y cells' behavior and differentiation has been investigated. Eumelanin-coated and uncoated PLA fibers proved biocompatible and supported SH-SY5Y cells' growth and proliferation. Both coated and uncoated fibers were able to encourage cells to assume a spindle-shaped morphology. However, the presence of the eumelanin coating was crucial in further incentivizing cell spreading, indicating that eumelanin may encourage SH-SY5Y cells to actively explore their surroundings. The eumelanin coating was also essential in promoting cell alignment along the substrate main axis and in triggering SH-SY5Y cell maturation towards a more mature neuronal phenotype in basal conditions (without the addition of growth factors in the cell culture media). Indeed, SH-SY5Y cells cultured on eumelanin-coated fibers showed increased expression levels of the neuronal markers NeuN and GAP-43 as well as an increase in expression levels of the neuronal cytoskeletal proteins MAP-2 and βIII-tubulin, suggesting that SH-SY5Y cells maturation is accompanied by changes in the cytoskeletal organization which has to provide adequate support. Our work suggests that the chemical and topographical properties of a biologically-inspired scaffold can be effectively tuned to provide instructive cues to interfacing cells. These findings, together with eumelanin's physical-chemical properties and its ionic-to-electronic mixed conductivity, may shed new light on the use of melanin-based materials as bioinspired platforms for several biomedical applications, including neural tissue engineering, tissue regeneration, bioelectronics, and antioxidant therapy.

4. Experimental Section

Fibers Fabrication: Poly(lactic acid) (PLA) (Ingeo™ 4032D 0.7 mol% L-isomer, Mw = 2.1×10^5 g mol^{-1}, and the polydispersity (PDI) = 1.7) was supplied by NatureWorks LLC; all solvents were reagent grade. The PLA solution (10% w/v in chloroform/dimethylformamide 90/10) was electrospun through an electrospinning setup NF103 MECC Co., Ltd. (Fukuoka, Japan) at a flow rate and voltage described before by Fasolino et al. Highly aligned meshes were realized by gap electrospinning using a parallel electrode. Then different layers of electrospun meshes were stuck on a glass substrate (2 × 2 cm). Later, aligned microfibers were functionalized with eumelanin coating via spin coating starting from a DHI solution followed by the annealing at 30 °C for 30′ under a nitrogen atmosphere as reported in Fasolino et al.[35]

Fiber Density Analysis: Fiber density was calculated from SEM images; three images at 4000x magnification were used for density calculation. The "Cell Counter" feature in ImageJ was utilized to evaluate the fiber number within a fixed distance orthogonal to the fiber alignment direction. Then the fiber density was calculated as the number of fibers per length (#/μm).

In Vitro Cell Culture: SH-SY5Y cells were purchased from Sigma-Aldrich (Italy). Cells were cultured in Dulbecco's modified Eagle medium (DMEM), supplemented with 10% of fetal bovine serum (Life Technologies), an antibiotic solution (streptomycin 100 μg ml^{-1} and penicillin 100 U ml^{-1}, Sigma Chem. Co) and 2 mM L-glutamine. Cells were grown in an incubator at 37 °C, 95% relative humidity, and a 5% CO_2 atmosphere. Cells were seeded onto the microfibers with and without eumelanin coating and were maintained in culture for up to 21 days. The cell culture medium was changed every 3 days. Substrates sterilization was performed under UV light for 2 h.

Live/Dead Assay: Cells were seeded on glass, PLA, and EU@PLA fibers at a density of 40 000 cells cm^{-2} and incubated at 37 °C with 5% CO_2. Cytotoxicity was evaluated after 1 DIV using Calcein-AM (Sigma-Aldrich) to fluorescently label live cells and ethidium homodimer (Abcam to fluorescently label dead cells). The staining solution containing 1 μg mL^{-1} Calcein AM and 1 μg mL^{-1} ethidium homodimer was added to cells and incubated for 15 min at 37 °C. Samples were rinsed in PBS and mounted on glass coverslips for imaging. Images were collected with an epi-fluorescence microscope (Axio Imager Z2 Vario, Zeiss) using an N-Achroplan" 20x/0.5 water objective with an additional Optovar 1.6x magnification. Numbers of live and dead cells were counted using the "Find Maxima" command on ImageJ. The percentage of live cells was measured using the following formula:

$$\%Viability = \frac{(Live\,cells)}{(Live\,cells + Dead\,cells)} \times 100 \qquad (1)$$

Viability was determined by acquiring 5 frames per experiment from three independent cell preparations. These were collected randomly over the material surface. Each experimental condition was studied in triplicate ($n = 3$).

Proliferation Assay: Biological investigations aimed to test the effect of eumelanin-coated microfibers on cell viability were performed by seeding 1.5×10^4 viable cells/well onto microfibers using a 48-well plate. Cells seeded in plates were used as control. At different time points (DIV 1, DIV 7, DIV 14, and DIV 21), the cell culture medium was removed, and cells were incubated with an Alamar blue solution in order to check cell survival. Specifically, Alamar Blue^{TM} (Sigma-Aldrich) solution was directly added to each well and incubated at 37 °C for 4 h to detect cell metabolism expressed as mitochondrial reductase activity. Mitochondrial reductase conversion of resazurin to resorufin was measured as optical density with a spectrophotometer (BioTeK® Synergy MX, Winooski, VT, USA) at wavelengths of 570 and 600 nm.

Immunocytochemistry: Cells were plated onto substrates placed in a 6 Multiwell plate (2.5×10^4 cells/well) or on glass control. For the cell alignment experiments, cells were fixed at DIV 7 with a solution of 4% (w/v) paraformaldehyde (PFA) (Sigma-Aldrich) for 20 min at RT, permeabilized in 0.1% Triton (Sigma-Aldrich) for 10 minutes and then incubated in a blocking solution containing 5% (v/v) donkey serum (Sigma-Aldrich) in Phosphate Buffered Saline (PBS) for 1 h. Cells were then labeled with FITC-conjugated phalloidin (1:200 Sigma-Aldrich) for 30′ at RT (room temperature). Nuclei were counterstained with 4′,6-diamidino-2-phenylindole (DAPI) at a concentration of 10 μg mL^{-1} for 10 min at 37 °C for nuclei detection and mounted with Fluoromount^{TM} (Sigma-Aldrich) mounting medium. Cells were observed under a wide field fluorescent microscope (July stage microscope, Nanoentek) or using a confocal laser-scanning microscope at magnification 10x (Leica TCS SP8 confocal microscope, Germany).

For the cell maturation experiment, cells were fixed at DIV 21 with a solution of 4% (w/v) paraformaldehyde (PFA) (Sigma-Aldrich) for 20 min at RT, permeabilized in 0.1% Triton (Sigma-Aldrich) for 10 min and then incubated in a blocking solution containing 5% (v/v) donkey serum (Sigma-Aldrich) in phosphate buffered saline (PBS) for 1 h. Cells were then labeled with FITC-conjugated Gap-43 (1:100 dilution) overnight at 4 °C. After washing the samples three times with PBS for 15 min, rhodamine-conjugated phalloidin (1:200 Sigma-Aldrich) was for

30' at RT (room temperature). Finally, the incubation for 10 min at 37 °C with DAPI (for nuclei detection) was performed. The cells were again washed with PBS thrice to remove any excess staining. The samples were then removed and mounted over glass slides. The glass slides were observed using confocal laser scanning microscopy at magnification 10X (Leica TCS SP8 confocal microscope, Germany).

For the visualization of the cytoskeleton, cells were labeled with microtubule-associated protein (MAP2) rabbit polyclonal antibody (1:200, SYSY) and for β-III tubulin mouse monoclonal antibody (1:200, Abcam). Both antibodies were diluted in 1% BSA in PBS and incubated with cells for 60 minutes at room temperature. Samples were washed three times in 1% BSA in PBS and labeled with Alexa Fluor 488 goat anti-rabbit secondary antibody (1:500, Abcam) and Alexa Fluor 647 goat anti-mouse secondary antibody (1:500, Invitrogen). Both antibodies were diluted in 1% BSA in PBS for 60 min at room temperature; cells were then washed three times in 1% BSA in PBS. Cell nuclei were stained with Hoechst in 1% BSA in PBS (1:5000, Life Technologies) for 10 min at room temperature. Samples were washed three times in PBS and imaged. Images were collected with an epi-fluorescence microscope (Axio Imager Z2 Vario, Zeiss) using an N-Achroplan" 40x/0.75 water objective with an additional Optovar 1.6x magnification.

Sample Preparation for Electron and Ion Microscopy: Samples were prepared following the ultra-thin plasticization procedure.[65,66] First, the biological samples were chemically fixed in 4% v/v paraformaldehyde dissolved in water milli-Q, then in 2.5% v/v glutaraldehyde (Electron Microscopy Science) diluted in 0.1 M cacodylate buffer (Electron Microscopy Science) overnight at 4 °C. Subsequently, samples were washed with a 0.1 M cacodylate solution. During these steps, the samples were kept on ice.

The buffer solution was then replaced with 20 mM Glycine (prepared in sodium cacodylate 0.1 M) and kept for 20 min. Afterward, the samples were incubated in a solution with 4% v/v aqueous osmium tetroxide (Electron Microscopy Science) and 2% potassium ferrocyanide (Electron Microscopy Science) for 1 h at 4 °C, away from direct light. Samples were then washed three times with 0.1 M cacodylate buffer solution. A final incubation with 2% v/v osmium tetroxide (Electron Microscopy Science) aqueous solution was performed at room temperature for 30 min. Carefully, the specimens were rinsed with DI water at room temperature and then immersed in 1% filtered thiocarbohydrazide (TCH, Electron Microscopy Science) in DI water for 20 min at room temperature. Subsequently, the samples were washed three times in DI water, and then they were incubated overnight at 4 °C en bloc staining solution in 4% v/v uranyl acetate. Afterward, they were rinsed again three times with DI water and then kept in 0.15% v/v tannic acid solution (Sigma Aldrich), for 3 min at 4 °C. The dehydration was carried out in a series of ethanol dilutions (30% v/v, 50% v/v, 75% v/v, 2×95% v/v, 100% v/v, ethanol in water) for 10 min at 4 °C. In addition, 100% ethanol was exchanged twice at room temperature. Finally, the samples were gradually embedded in resin (25 mL of NSA, 8 mL D.E.R. 736, 10 mL of ERL 4221, 301 μL of DMAE, Electron Microscopy Science) with different ethanol:resin ratios. The first embedding was in ethanol: resin with a ratio of 1:3 and the sample was kept embedded for 2 h. While the second ratio used was 1:2, for 2 h and then, the last embedding was in absolute resin kept overnight and day. Therefore, the specimens were put in a vertical position for 3 h and then polymerized for 24 h at 70 °C. Samples were mounted onto aluminum stubs (diameter = 3.2 mm) using silver conductive paste (RS Pro) and sputtered with a 20 nm thick golden layer prior to imaging.

Scanning Electron Microscopy: SEM imaging was carried out using an FEI Quanta 600 field emission gun (FEG) SEM. The samples were imaged with acceleration voltages in the range of 3 kV and a working distance of 5–7 mm.

Scanning Electron Microscopy – Focused Ion Beam: The specimens were loaded inside the dual-beam vacuum chamber (Thermo Fischer, Helios NanoLab 600i and 650). The region of interest (ROI) was detected. Two deposition layers were performed, firstly an electron beam deposition (0.5 μm thickness of platinum, with current 11nA and tension 3 kV); then the ion beam deposition (0.5 μm thickness of platinum, with current 0.43 nA and tension 30 kV). Cross sections were performed by first trenching out the material via an ion beam (cutting thickness: 3 μm; current: 0.79nA; tension: 30 kV). The ion beam was then used to polish the interface (current: 0.23–0.43 nA; tension: 30 kV). Scanning electron micrographs were acquired in backscattered mode with a dwell time of 10 μs and the electron beam to 3 kV and 0.17–0.69 nA.

Morphology Analysis: Morphological characteristics were investigated through the assessment of different parameters: the shape factor, defined as $4\pi A/P^2$, where A is the area and P is the perimeter of the cell; the elliptical form factor (EFF), defined as the major axis divided by the minor axis, and the average area of cell spreading. The cell area and perimeter, as well as the length of the minor and major axes, were measured via ImageJ based on the captured SEM micrographs of SH-SY5Y cells on PLA and EU@PLA fibers at DIV 7 and DIV 21.

Alignment Analysis: For the alignment analysis, the "Directionality" plugin on ImageJ, based on the Fast Fourier Transform algorithm, was used to determine the pixel directionality of the cells in each image. The computation of the algorithm was set on 180 bins, producing a directionality histogram of 180°.

Fluorescence Intensity Analysis: Images were analyzed in ImageJ (ImageJ 1.44 which uses Java 1.6 in 64-bit mode) in order to compare fluorescence intensity. Fluorescence intensity was calculated by subtracting the cell intensity from the background intensity and normalizing to the number of cells per frame.

Statistical Analysis: Three parallel cultures were prepared for each substrate and every experiment was repeated three times ($n = 3$). The statistical analysis was performed using GraphPad Prisms 8. For the viability assay, a one-way ANOVA test followed by a Dunnett's post hoc analysis was performed to assess any effect of the substrates used on the percentage of live cells compared to glass. For the proliferation assay, a one-way ANOVA test followed by a Dunnett's post hoc analysis was performed to assess any substrate-mediated effect on cell proliferation compared to glass across all culture times investigated. The substrate-mediated changes in morphology were compared using an unpaired Student's t-test at both DIV 7 and DIV 21. The level of expressions of neuronal markers for the cell differentiation experiment was compared using an unpaired Student's t-test. Significance was established at p-value < 0.05.

Supporting Information

Supporting Information is available from the Wiley Online Library or from the author.

Acknowledgements

Conflict of Interest

The authors declare no conflict of interest.

Data Availability Statement

The data that support the findings of this study are available from the corresponding author upon reasonable request.

Keywords

bioelectronics, biomimetic fibers, eumelanin, neural tissue engineering, neuronal differentiation

[1] G. M. Artmann, S. Chien, *Bioengineering in Cell and Tissue Research*, Springer, Heidelberg **2008**.

[2] L. R. Doblado, C. Martínez-Ramos, M. M. Pradas, *Front. Nanotechnol.* **2021**, *3*, 643507.

[3] R. Boni, A. Ali, A. Shavandi, A. N. Clarkson, *J. Biomed. Sci.* **2018**, *25*, 90.

[4] A. Mariano, C. Lubrano, U. Bruno, C. Ausilio, N. B. Dinger, F. Santoro, *Chem. Rev.* **2021**, *122*, 4552.

[5] C. J. Bettinger, R. Langer, J. T. Borenstein, *Angew. Chem., Int. Ed.* **2009**, *48*, 5406.

[6] M. K. Driscoll, X. Sun, C. Guven, J. T. Fourkas, W. Losert, *ACS Nano* **2014**, *8*, 3546.

[7] D. Hoffman-Kim, J. A. Mitchel, R. V. Bellamkonda, *Annu. Rev. Biomed. Eng.* **2010**, *12*, 203.

[8] A. Mariano, C. L. Bovio, V. Criscuolo, F. Santoro, *Nanotechnology* **2022**, *33*, 492501.

[9] Y. Hu, H. Zhang, H. Wei, H. Cheng, J. Cai, X. Chen, L. Xia, H. Wang, R. Chai, *Eng. Regener.* **2022**, *3*, 154.

[10] W. Xue, W. Shi, Y. Kong, M. Kuss, B. Duan, *Bioact. Mater.* **2021**, *6*, 4141.

[11] J. Zhang, X. Zhang, C. Wang, F. Li, Z. Qiao, L. Zeng, Z. Wang, H. Liu, J. Ding, H. Yang, *Adv. Healthcare Mater.* **2021**, *10*, 2000604.

[12] K. Liu, L. Yan, R. Li, Z. Song, J. Ding, B. Liu, X. Chen, *Adv. Sci.* **2022**, *9*, 2103875.

[13] X. Zhang, W. Qu, D. Li, K. Shi, R. Li, Y. Han, E. Jin, J. Ding, X. Chen, *Adv. Mater. Interfaces* **2020**, *7*, 2000225.

[14] J. Ding, J. Zhang, J. Li, D. Li, C. Xiao, H. Xiao, H. Yang, X. Zhuang, X. Chen, *Prog. Polym. Sci.* **2019**, *90*, 1.

[15] M. C. Amores de Sousa, C. A. V. Rodrigues, I. A. F. Ferreira, M. M. Diogo, R. J. Linhardt, J. M. S. Cabral, F. C. Ferreira, *Front. Bioeng. Biotechnol.* **2020**, *8*, 580135.

[16] J.-M. Bourget, F. A. Auger, L. Germain, M. Guillemette, T. Veres, *In Advances in Biomaterials Science and Biomedical Applications*, (Ed.: R. Pignatello), InTechOpen, London **2013**.

[17] J. Slavík, V. Čmiel, J. Hubálek, Y. Yang, T.-L. Ren, *Appl. Sci.* **2020**, *11*, 275.

[18] S. H. Lim, X. Y. Liu, H. Song, K. J. Yarema, H.-Q. Mao, *Biomaterials* **2010**, *31*, 9031.

[19] K. Lee, E. H. Kim, N. Oh, N. A. Tuan, N. H. Bae, S. J. Lee, K. G. Lee, C.-Y. Eom, E. K. Yim, S. Park, *J. Nanobiotechnol.* **2016**, *14*, 35.

[20] F. Yang, R. Murugan, S. Wang, S. Ramakrishna, *Biomaterials* **2005**, *26*, 2603.

[21] S. G. Kumbar, S. P. Nukavarapu, R. James, L. S. Nair, C. T. Laurencin, *Biomaterials* **2008**, *29*, 4100.

[22] Y. Ji, K. Ghosh, X. Shu, B. Li, J. Sokolov, G. Prestwich, R. Clark, M. Rafailovich, *Biomaterials* **2006**, *27*, 3782.

[23] L. C. Lins, F. Wianny, S. Livi, I. A. Hidalgo, C. Dehay, J. Duchet-Rumeau, J.-F. Gérard, *Biomacromolecules* **2016**, *17*, 3172.

[24] T. Sudwilai, J. J. Ng, C. Boonkrai, N. Israsena, S. Chuangchote, P. Supaphol, *J. Biomater. Sci., Polym. Ed.* **2014**, *25*, 1240.

[25] J. Zhou, Y. Wang, L. Cheng, Z. Wu, X. Sun, J. Peng, *Neural Regen. Res.* **2016**, *11*, 1644.

[26] D. T. Simon, E. O. Gabrielsson, K. Tybrandt, M. Berggren, *Chem. Rev.* **2016**, *116*, 13009.

[27] M. d'Ischia, A. Napolitano, A. Pezzella, P. Meredith, T. Sarna, *Angew. Chem., Int. Ed.* **2009**, *48*, 3914.

[28] M. d'Ischia, K. Wakamatsu, F. Cicoira, E. Di Mauro, J. C. Garcia-Borron, S. Commo, I. Galván, G. Ghanem, K. Kenzo, P. Meredith, A. Pezzella, C. Santato, T. Sarna, J. D. Simon, L. Zecca, F. A. Zucca, A. Napolitano, S. Ito, *Pigm. Cell Melanoma Res.* **2015**, *28*, 520.

[29] X. Liu, J. Cao, H. Li, J. Li, Q. Jin, K. Ren, J. Ji, *ACS Nano* **2013**, *7*, 9384.

[30] H. Wei, J. Ren, B. Han, L. Xu, L. Han, L. Jia, *Colloids Surf., B* **2013**, *110*, 22.

[31] C. J. Bettinger, J. P. Bruggeman, A. Misra, J. T. Borenstein, R. Langer, *Biomaterials* **2009**, *30*, 3050.

[32] A. Pezzella, M. Barra, A. Musto, A. Navarra, M. Alfè, P. Manini, S. Parisi, A. Cassinese, V. Criscuolo, M. d'Ischia, *Mater. Horiz.* **2015**, *2*, 212.

[33] L. Migliaccio, S. Aprano, L. Iannuzzi, M. G. Maglione, P. Tassini, C. Minarini, P. Manini, A. Pezzella, *Adv. Electron. Mater.* **2017**, *3*, 1600342.

[34] V. Gargiulo, M. Alfè, R. D. Capua, A. R. Togna, V. Cammisotto, S. Fiorito, A. Musto, A. Navarra, S. Parisi, A. Pezzella, *J. Mater. Chem. B* **2015**, *3*, 5070.

[35] I. Fasolino, I. Bonadies, L. Ambrosio, M. G. Raucci, C. Carfagna, F. M. Caso, F. Cimino, A. Pezzella, *ACS Appl. Mater. Interfaces* **2017**, *9*, 40070.

[36] A. Niaz, J. Karunia, M. Mandwie, K. A. Keay, G. Musumeci, G. Al-Badri, A. Castorina, *J. Mol. Neurosci.* **2021**, *71*, 565.

[37] A. F. Abouraddy, M. Bayindir, G. Benoit, S. D. Hart, K. Kuriki, N. Orf, O. Shapira, F. Sorin, B. Temelkuran, Y. Fink, *Nat. Mater.* **2007**, *6*, 336.

[38] S. Hou, P. Lu, *Neural Regen. Res.* **2016**, *11*, 1824.

[39] K. Langfelder, M. Streibel, B. Jahn, G. Haase, A. A. Brakhage, *Fungal Genet. Biol.* **2003**, *38*, 143.

[40] D. C. Montefiori, J. Zhou, *Antiviral Res.* **1991**, *15*, 11.

[41] B. S. Larsson, *Pigment Cell Res.* **1993**, *6*, 127.

[42] J. V. Paulin, C. F. O. Graeff, *J. Mater. Chem. C* **2021**, *9*, 14514.

[43] I. Bonadies, F. Cimino, C. Carfagna, A. Pezzella, *Biomacromolecules* **2015**, *16*, 1667.

[44] D. da Silva, M. Kaduri, M. Poley, O. Adir, N. Krinsky, J. Shainsky-Roitman, A. Schroeder, *Chem. Eng. J.* **2018**, *340*, 9.

[45] X. Li, X. Wang, D. Yao, J. Jiang, X. Guo, Y. Gao, Q. Li, C. Shen, *Colloids Surf., B* **2018**, *171*, 461.

[46] E. Soliman, F. Bianchi, J. N. Sleigh, J. H. George, M. Z. Cader, Z. Cui, H. Ye, *Biotechnol. Lett.* **2018**, *40*, 601.

[47] S. Cai, C. Wu, W. Yang, W. Liang, H. Yu, L. Liu, *Nanotechnol. Rev.* **2020**, *9*, 971.

[48] S. Ferraris, S. Spriano, A. C. Scalia, A. Cochis, L. Rimondini, I. Cruz-Maya, V. Guarino, A. Varesano, C. Vineis, *Polymers* **2020**, *12*, 2896.

[49] V. Cirillo, V. Guarino, M. A. Alvarez-Perez, M. Marrese, L. Ambrosio, *J. Mater. Sci.: Mater. Med.* **2014**, *25*, 2323.

[50] J.-C. Chang, S. Fujita, H. Tonami, K. Kato, H. Iwata, S. Hsu, *Biomed. Mater.* **2013**, *8*, 055002.

[51] B. Yi, Y. Shen, H. Tang, X. Wang, B. Li, Y. Zhang, *ACS Appl. Mater. Interfaces* **2019**, *11*, 6867.

[52] C. A. Heckman, H. K. Plummer, *Cell Signal* **2013**, *25*, 2298.

[53] S. L. Gupton, F. B. Gertler, *Sci. STKE* **2007**, *2007*, re5.

[54] Guillaume Jacquemet, Hellyeh Hamidi, Johanna Ivaska, *Prog. Polym. Sci.* **2015**, *36*, 23.

[55] M. L. Hendrickson, A. J. Rao, O. N. A. Demerdash, R. E. Kalil, *PLoS One* **2011**, *6*, 18535.

[56] R. Constantinescu, A. T. Constantinescu, H. Reichmann, B. Janetzky, in *Neuropsychiatric Disorders: An IntegrativeApproach*, (Eds.: M. Gerlach, J. Deckert, K. Double, E. Koutsilieri), Springer, Vienna **2007**, p. 17–28.

[57] V. V. Gusel'nikova, D. E. Korzhevskiy, *Acta Naturae* **2015**, *7*, 42.

[58] M. Encinas, M. Iglesias, Y. Liu, H. Wang, A. Muhaisen, V. Ceña, C. Gallego, J. X. Comella, *J. Neurochem.* **2002**, *75*, 991.

[59] S. Påhlman, A.-I. Ruusala, L. Abrahamsson, M. E. K. Mattsson, T. Esscher, *Cell Differ.* **1984**, *14*, 135.

[60] J. Kovalevich, D. Langford, in *Neuronal Cell Culture*, (Eds.: S. Amini, M. K. White), Humana Press, Totowa, NJ **2013**, p. 9–21.

[61] L. I. Benowitz, A. Routtenberg, *Trends Neurosci.* **1997**, *20*, 84.

[62] S. Gianola, F. Rossi, *Eur. J. Neurosci.* **2004**, *19*, 819.

[63] M. Lasser, J. Tiber, L. A. Lowery, *Front. Cell Neurosci.* **2018**, *12*, 165.

[64] A. Matus, R. Bernhardt, R. Bodmer, D. Alaimo, *Neuroscience* **1986**, *17*, 371.

[65] F. Santoro, W. Zhao, L.-M. Joubert, L. Duan, J. Schnitker, Y. van de Burgt, H.-Y. Lou, B. Liu, A. Salleo, L. Cui, Y. Cui, B. Cui, *ACS Nano* **2017**, *11*, 8320.

[66] A. Belu, J. Schnitker, S. Bertazzo, E. Neumann, D. Mayer, A. Offenhäusser, F. Santoro, *J. Microsc.* **2016**, *263*, 78.